HHS Public Access

Author manuscript

Br J Pharmacol. Author manuscript; available in PMC 2023 June 01.

Published in final edited form as:

Br J Pharmacol. 2022 June ; 179(12): 2953–2968. doi:10.1111/bph.15779.

Crosstalk between ENaC and basolateral $K_{ir}4.1/K_{ir}5.1$ channels in the cortical collecting duct

Elena Isaeva[1,3], **Ruslan Bohovyk**[1,3,8], **Mykhailo Fedoriuk**[1,3], **Alexey Shalygin**[1,6], **Christine A. Klemens**[1,2,8], **Adrian Zietara**[1,8], **Vladislav Levchenko**[1,8], **Jerod S. Denton**[5], **Alexander Staruschenko**[1,2,4,8], **Oleg Palygin**[1,7]

[1]Department of Physiology, Medical College of Wisconsin, Milwaukee, WI 53226, USA

[2]Cardiovascular Center, Medical College of Wisconsin, Milwaukee, WI 53226, USA

[3]Department of Cellular Membranology, Bogomoletz Institute of Physiology, Kyiv, Ukraine

[4]Clement J. Zablocki VA Medical Center, Milwaukee, WI 53295, USA

[5]Department of Anesthesiology and Pharmacology, Vanderbilt University Medical Center, Nashville, TN 37232, USA

[6]Institute of Cytology of the Russian Academy of Sciences, St. Petersburg, Russia

[7]Department of Medicine, Division of Nephrology, Medical University of South Carolina, Charleston, SC 29425, USA

[8]Department of Molecular Pharmacology and Physiology, University of South Florida, Tampa, FL 33602, USA

Abstract

Background and Purpose: Inwardly rectifying K^+ (K_{ir}) channels located on the basolateral membrane of epithelial cells of the distal nephron play a crucial role in K^+ handling and blood pressure control, making these channels an attractive target for the treatment of hypertension. The purpose of the present study was to determine how the inhibition of basolateral $K_{ir}4.1/K_{ir}5.1$ heteromeric K^+ channel affects epithelial sodium channel (ENaC)-mediated Na^+ transport in the principal cells of cortical collecting duct (CCD).

Experimental Approach: The effect of fluoxetine, amitriptyline, and recently developed K_{ir} inhibitor, VU0134992, on the activity of $K_{ir}4.1$, $K_{ir}4.1/K_{ir}5.1$, and ENaC were tested using electrophysiological approaches in Chinese hamster ovary (CHO) cells transfected with respective channel subunits, cultured polarized epithelial $mCCD_{cl1}$ cells, and freshly isolated rat and human CCD tubules. To test the effect of pharmacological $K_{ir}4.1/K_{ir}5.1$ inhibition on electrolyte

Correspondence: Oleg Palygin, PhD; Department of Medicine, Division of Nephrology, Medical University of South Carolina, 70 President St, DD508, Charleston, SC 29425, USA. Phone: (843) 792 4307; palygin@musc.edu.

Author contributions:

EI, JD, ASt, and OP designed the study; EI, RB, MF, ASh, CK, AZ, and VL carried out experiments; EI, RB, MF, ASh, and OP, analyzed the data; JD contributed novel compound; EI, ASh, and OP prepared the figures; EI, ASt, and OP drafted and revised the paper. All authors approved the final version of the manuscript.

Conflict of interest disclosure: The authors declare no competing interests.

homeostasis *in vivo* and corresponding changes in distal tubule transport, Dahl salt-sensitive rats were injected with amitriptyline (15 mg kg^{-1} day^{-1}) for three days.

Key Results: We found that inhibition of $K_{ir}4.1/K_{ir}5.1$, but not $K_{ir}4.1$ channel, depolarizes cell membrane, induces the elevation of intracellular Ca^{2+} concentration, and suppresses ENaC activity. Furthermore, we demonstrate that amitriptyline administration leads to a significant drop in plasma K^+ level, triggering sodium excretion and diuresis.

Conclusion and Implications: Present data uncovers a specific role of the $K_{ir}4.1/K_{ir}5.1$ channel in the modulation of ENaC activity and emphasizes the potential for using $K_{ir}4.1/K_{ir}5.1$ inhibitors to regulate electrolyte homeostasis and blood pressure.

Keywords

Kcnj10; Kcnj16; hypokalemia; amitriptyline; K_{ir} (IRK) channels; ENaC

1 | INTRODUCTION

According to the Centers for Disease Control and Prevention and the American Heart Association, nearly one-third of the adult population in the United States has hypertension, which is a leading risk factor for cardiovascular disease, stroke, kidney failure, and all-cause mortality (Virani et al., 2020). Observational studies and treatment trials provide strong support for a link between excess dietary Na^+ intake and the incidence of hypertension. The effect of Na^+ on blood pressure is dependent on diet composition, specifically on the ratio of Na^+ and K^+ ions (Staruschenko, 2018). The beneficial effects of a potassium-enriched diet for blood-pressure control are supported by animal studies and human trials (Dahl et al., 1972; Mente et al., 2014; Tobian, 1991). Understanding the regulatory machinery involved in the interplay between Na^+ and K^+ homeostasis is a vital milestone to develop an appropriate therapy to prevent hypertension and related cardiovascular and renal disorders.

The aldosterone-sensitive distal nephron (ASDN) plays an essential role in the control of the pressure–natriuresis relationship and long-term regulation of blood pressure. Urinary Na^+/water reabsorption and K^+ excretion in this region are tightly interconnected and controlled by various channels and transporters expressed in the apical and basolateral membranes of epithelial cells along ASDN. Recent genetic human and animal studies uncovered the critical role of basolateral Kir channels, specifically monomeric Kir4.1 (encoded by Kcnj10 gene) and heteromeric $K_{ir}4.1$/Kir5.1 (encoded by *Kcnj10* and *Kcnj16*), of the ASDN to control electrolyte homeostasis and blood pressure. Loss-of-function mutations in the genes encoding $K_{ir}4.1$ are associated with salt-wasting, hypotension, and severe hypokalemia in both human and animal models (Bockenhauer et al., 2009; Cuevas et al., 2017). Recent studies further identified several mutations in *KCNJ16* encoding $K_{ir}5.1$, which result in hypokalemia, salt-wasting, and disturbed acid-base homeostasis (Schlingmann et al., 2021). Deletion of *Kcnj16* in Dahl salt-sensitive (SS) rats ($SS^{Kcnj16-/-}$) targeting heteromeric $K_{ir}4.1/K_{ir}5.1$ channel, a major basolateral K_{ir} channel in ASDN, results in a renal phenotype resembling distinctive features of human and murine loss of function $K_{ir}5.1$ mutations, including hypokalemia and reduced blood pressure (Manis et al., 2019; Palygin et al., 2017; Schlingmann et al., 2021) providing evidence that modulation of $K_{ir}4.1/K_{ir}5.1$ channel

activity may be a powerful tool for blood pressure and hyperkalemia control in salt-induced hypertension.

The use of genetically modified rodent models provides important insight into the mechanisms of human diseases, but the interpretation of these data is generally complicated due to the possible existence of compensatory mechanisms. The aim of the present study was to dissect the effect of pharmacological inhibition of homomeric $K_{ir}4.1$ and heteromeric $K_{ir}4.1/K_{ir}5.1$ channels on the epithelial sodium channel (ENaC) activity in CCD using overexpressed cells, cell culture, and freshly isolated tubules from Dahl SS rat and human kidneys. Using established and newly discovered inhibitors of basolateral K_{ir} channels, amitriptyline, fluoxetine, and VU0134992, we demonstrated that acute inhibition of $K_{ir}4.1/K_{ir}5.1$ channel but not $K_{ir}4.1$ induces suppression of ENaC activity in rodent and human CCD principal cells. The suppression of ENaC activity is presumably mediated by the cell depolarization and increase in cytosolic free Ca^{2+} concentration. We also show that similar to the results obtained in $SS^{Kcnj16-/-}$ rats, the injection of SS rats by amitriptyline promotes a significant decline in blood K^+ level and induces salt excretion despite the upregulation of renal sodium-chloride co-transporter.

2 | METHODS

2.1 | Experimental animals and human kidneys (Compliance with requirements for studies using animals and human tissue)

To fully test our hypothesis, some experiments in our study were performed in whole animals and in the tissue of highly-differentiated cells that contain native K_{ir} channels and retain their physiological function, that cannot be fully replicated by cell lines. All animal studies were conducted in accordance with the National Institutes of Health Guide for the Care and Use of Laboratory Animals following protocol review and approval by the Institutional Care and Use Committee of the Medical College of Wisconsin. Animal studies are reported in compliance with the ARRIVE guidelines and with the recommendations made by the British Journal of Pharmacology (Lilley et al., 2020; McGrath & Lilley, 2015). The re-derived Rapp Dahl salt-sensitive (SS; RRID:RGD_69369) rat used in our studies (SS/JrHsdMcwi) has been inbred for more than 50 generations at the Medical College of Wisconsin and used to compare the outcomes of pharmacological inhibition of K_{ir} channels with results obtained earlier in the same SS strain with a null mutation of *Kcnj16* (Manis et al., 2021; Manis et al., 2019; Palygin et al., 2017). 8-12-week-old male SS rats (TBW approx. 220 g) were used. Animals were kept in standard plastic home cages (Allentown 40 IVC) on hardwood chip bedding. For urine collection, animals were moved into metabolic cages (# 40615; Laboratory Products, one animal per cage). Rats were maintained on a standard 12/12 hrs light-dark cycle with unlimited access to water and rodent chow (0.4% NaCl, 0.36% K, # D113755, Dyets Inc., Bethlehem, PA).

Studies in this manuscript that involve human kidneys are not considered “human subjects research” for the purpose of addressing human subject protection because they are only secondary analysis of coded discarded organs, and none of the investigators can readily ascertain the identity of subjects. MCW IRB Committee reviewed current studies and determined that it does not meet criteria for human subject research since information is

not individually identifiable and it does not involve intervention or interaction with living individuals. For experiments with human tissue, human kidneys (no patient identifiers were received) were obtained from an organ procurement company, where they were harvested with the intent to be used for transplantation but were not used and destined to be discarded. The kidneys were stored in a transplant preservation UW solution (ViaSpan) on ice before the isolation of nephron segments by vibrodissociation technique as described (Isaeva et al., 2019; Khedr et al., 2019).

2.2 | Isolation of renal tubules

Animals were deeply anesthetized with 5% isoflurane in 30% O_2/70% N_2, and kidneys were harvested. Thereafter rats were humanely euthanized by a thoracotomy. Kidneys were extensively washed in the incubation solution contained (in mM): 119 NaCl, 4.5 KCl, 2 $CaCl_2$, 1.3 $MgCl_2$, 26 $NaHCO_3$, 1.2 NaH_2PO_4, 5 glucose (pH = 7.35). Both human and rodent kidneys were manually cut into slices (0.5–1 mm thickness) and stored at room temperature in oxygenated incubation solution (95% O_2 - 5% CO_2) contained (in mM): 119 NaCl, 4.5 KCl, 2 $CaCl_2$, 1.3 $MgCl_2$, 26 $NaHCO_3$, 1.2 NaH_2PO_4, 5 glucose (pH = 7.35). For renal tubule separation, kidney slices were enzymatically pretreated for 20–25 min at 37°C in physiological saline solution (PSS) of the following composition (in mM) 150 NaCl, 5 KCl, 1 CaCl2, 2 MgCl2, 5 glucose, and 10 HEPES pH=7.35) containing 0.7 mg ml^{-1} collagenase type I (Alfa Aesar, Ward Hill, MA) and 4 mg ml^{-1} of dispase II (Roche Diagnostics, Mannheim, Germany). After enzymatic treatment, slices were extensively washed in PSS and dissociated by applying a local mechanical vibration movement towards the slice surface using a flame-sealed glass micropipette connected to a frequency oscillator (GFG-8250A, Instek).

2.3 | Chinese hamster ovary (CHO) cell culture and transfection

CHO (RRID:CVCL_0213) cells were obtained from American Type Culture Collection (ATCC; Manassas, VA, USA) and maintained under standard culture conditions (F12K medium supplemented with 10% fetal bovine serum, 100 U ml^{-1} penicillin, and 100 μg ml^{-1} streptomycin) as previously described (Staruschenko et al., 2005). In transfection experiments, the cells were trypsinized, plated into 35-mm tissue culture dishes with coverslips, and grown for 20–24 hrs prior to transfection with Lipofectamine (Thermo Fisher Scientific). For expression of *Kcnj* in CHO cells, the cells were transiently cotransfected with green fluorescent protein (eGFP) (0.25 μg of cDNA/35-mm dish) and channel plasmids: *Kcnj10* (0.5 μg) for homomer expression or *Kcnj10* and *Kcnj16* (0.25 μg each) for heteromer expression. *Kcnj10* and *Kcnj16* plasmids were kindly provided by Dr. Richard Warth from the Institute of Physiology, Regensburg, Germany (Reichold et al., 2010). For expression of ENaC in CHO cells, subunits of α-, β-, γ-ENaC cDNA transfection ratios of 1:1:1 were used (0.3 μg of each cDNA/35-mm dish). To identify transfected cells, 0.5 μg of eGFP was also added to the cDNA mix. After transfection, cells were cultured on coverslips for 24–48 hours, and GFP-positive cells were selected for measurements.

2.4 | Mouse cortical collecting duct ($mCCD_{cl1}$) cell culture and short-circuit current (I_{eq}) measurements

$mCCD_{cl1}$ cells (Gaeggeler et al., 2005) were provided by Prof. Bernard Rossier (University of Lausanne, Switzerland) and were cultured in 75-cm flasks in Dulbecco's Minimum Essentials Medium (DMEM/F-12; Cat #11330, Gibco) supplemented with 2% Fetal Bovine Serum (FBS), 5 μg ml^{-1} insulin, 5 μg ml^{-1} human apo-Transferrin, 10 ng ml^{-1} epidermal growth factor (EGF), 1 nM triiodo-L-thyronine Na^+ salt, 60 nM Na^+ selenite, 50 nM dexamethasone, 100 units ml^{-1} penicillin, and 100 μg ml^{-1} streptomycin as previously described (Gaeggeler et al., 2005; Pavlov et al., 2014). For patch-clamp studies, cells were seeded into 35 mm cell culture dishes on coverglass chips (5 × 5 mm) and experiments were performed 3–7 days after passage. Transepithelial voltage (Vt) and resistance (Rt) were measured using the Millicell Electrical Resistance System (Millipore) with dual Ag/AgCl pellet electrodes on the cells grow on Transwell permeable supports (Costar) to form polarized monolayers. Intact polarized monolayer formation exhibiting Rt greater than >1000 Ω cm^2 and Vt greater than >20 mV was used for experiments (Assmus et al., 2018; Mukherjee et al., 2017). The equivalent short circuit current (I_{eq}) values were calculated using Ohm's law. Relative current indicates normalized I_{eq} values. Apical application of 10 μM amiloride produced near zero drops of I_{eq} current, demonstrating that the recorded currents were attributable to ENaC. We did not observe significant changes in *Rt* within 2 hrs following drugs application.

2.5 | Electrophysiological studies

The single-channel activity was determined in cell-attached patches made under voltage-clamp configuration. Potassium channel and epithelial sodium channel (ENaC) activity were recorded either on CHO cells overexpressing corresponding channels or freshly isolated CCDs. Potassium channel activity was recorded from the basolateral membrane of principal CCD cells. To directly assess ENaC properties, CCDs were split open, and channel activity was recorded from the apical membrane of principal cells.

Data were acquired and subsequently analyzed with Axopatch 200B amplifier interfaced via a Digidata 1440A to a PC running the pClamp 10.6 suite of software (Molecular Devices; RRID:SCR_011323). The recordings were filtered with an 8-pole, low-pass Bessel filter LPF-8 (Warner Inst.) at 0.3 kHz and 0.1 kHz for potassium current and ENaC recordings, correspondently. Events were inspected visually before acceptance to ensure that patches contained activity consistent with the channel of interest and are not contaminated with other conductance. In paired experiments, single channel activity was analyzed over a span of 60–120 s for each experimental condition (over 100 number of open/close events) after a new steady-state was reached in response to a treatment. Automatically detected event histograms fit with single or multiple Gaussian distributions were used to determine unitary current amplitudes (Clampfit 10.3 software). Channel activity and *Po* were assessed using Clampfit 10.3 software (Molecular Devices). To calculate *Po* in paired experiments, *N* was fixed as the greatest number of active channels observed in control or experimental conditions. All electrophysiological experiments were performed at room temperature (22–24 °C). The patch pipettes were pulled with a horizontal puller (Sutter P-97; Sutter Inst.), and their resistances were ranged from 7 to 12 MΩ when filled with corresponding pipette

solution. All electrophysiological recordings were performed using PSS as extracellular solution (in mM) 150 NaCl, 5 KCl, 1 $CaCl_2$, 2 $MgCl_2$, 5 glucose, and 10 HEPES (pH 7.35). The single-channel activity of $K_{ir}4.1/K_{ir}5.1$ and $K_{ir}4.1$ channels was measured using patch pipettes filled with a solution of the following composition (in mM): 150 KCl, 2 $MgCl_2$, and 10 HEPES (pH 7.35). For the recording of ENaC activity, patch pipettes were filled with a solution of the following composition (in mM): 140 LiCl, 2 $MgCl_2$, and 10 HEPES (pH 7.35).

2.6. Western blotting

Western blotting has been conducted according to BJP Guidelines (Alexander et al., 2018). For the Western blotting analyses, animals were separated into two groups: amitriptyline and control. The first group was treated for three days with i.p. injections of 15 mg kg^{-1} amitriptyline, while age-matched control rats were treated with vehicle. Kidneys were harvested as it was described in Methods 2.2, flushed with PBS, excised, and cut in 1- to 2-mm slices under a binocular microscope with ×6 magnification. The approximate apical kidney cortex sections were carved and then diced into small pieces with a razor blade. Samples were pulse sonicated in GLB with a protease inhibitor cocktail (Roche) for 10 seconds and spin cleared at 10,000 g for 10 minutes. The resulting supernatant was subjected to PAGE, transferred onto nitrocellulose membrane (Millipore) for probing with antibodies (tNCC # 2430347, Millipore; pNCC # p1311-53 PhosphoSolutions; αENaC # spc-403, γENaC # spc-405 StressMarq), and subsequently visualized by enhanced chemiluminescence (ECL; Amersham Biosciences).

2.7. Confocal microscopy.

For confocal microscopy, $mCCD_{cl1}$ cells were cultured on glass chips (size 0) to develop monolayer. Cells were loaded either with 2 μl ml^{-1} FluoVolt™ dye and 10 μl ml^{-1} PowerLoad Concentrate for membrane potential monitoring, or with 1 μg ml^{-1}, Fluo8^{HT} AM (AAT Bioquest) for Ca^{2+} imaging studies in the culture media for 20–30 min and incubated in CO_2 incubator (37°C). After loading, chips with cells were rinsed twice with PSS and mounted into recording/perfusion chamber (Warner Instruments, Hamden, CT). Confocal imaging recordings were performed in PSS using the Nikon A1-R laser scanning confocal microscope system and analyzed using ImageJ 1.52i software (RRID:SCR_003070), as previously reported (Golosova et al., 2020).

2.7 | Urine/serum biochemistry measurement

Rats were placed in metabolic cages to acclimate for 24 hrs. Urine was collected over 24 hrs before (two consecutive days of vehicle injection) and after intra-peritoneal (i.p.) administration of amitriptyline (as indicated in 2.6. Western blotting). Blood was collected from the tail vein before animal placement into metabolic cages and 24 hrs after the last injection of amitriptyline. Blood and urine electrolytes, and creatinine levels were analyzed using the ABL800 FLEX analyzer immediately after collection. Creatinine clearance was estimated using the formula: creatinine clearance = (creatinine urine concentration, mmol l^{-1} × urine flow, ml hr^{-1})/creatinine serum concentration, mmol l^{-1}.

2.8 | Drugs

Fluoxetine hydrochloride (# 0927) and Amitriptyline hydrochloride (# 4456/50) were purchased from Tocris, VU0134992 (VU992) was synthesized at Vanderbilt University Medical Center as recently reported (Kharade et al., 2018). All other drugs were purchased from Sigma. All drugs were dissolved in PSS, except VU992, which was initially dissolved in DMSO and then added to aqueous solutions. PSS or DMSO (for VU992) were used as vehicle controls, correspondingly.

2.9 | Data analysis and statistics

The data and statistical analysis comply with the recommendations of the *British Journal of Pharmacology* on experimental design and analysis in pharmacology (Curtis et al., 2018; Curtis et al., 2015). The declared group size is the number of independent values, and that statistical analysis was done using these independent values. The statistical analysis was undertaken only for studies where each group size was at least n=5. The experiments on freshly isolated human tissue are subject to availability, so these datasets had limited n per group and were not subjected to statistical analysis. The studies were designed to generate groups of equal size for the small groups (n<20), using randomization and blinded analysis. For group size calculation, we assumed a type I error rate of 0.05 and statistical power of at least 85%, as previously reported with similar experimental designs. Determination or exclusion of outliners within datasets was not applied. We estimated the acute effect of VU992 and amitriptyline on single-channel activity at 5 min following drugs application when the magnitude of the effect has reached its steady-state level.

Data are expressed as the mean ± SE of the mean, and data analysis for all protocols was performed blinded by an independent analyst. Data were tested for normality (Shapiro-Wilk) and equal variance (Levene's homogeneity test). Paired t-test was used to detect the statistical difference between two variables for the same subject. For more than two groups of variables for the same subject, the repeated measurements (RM) ANOVA was used with corresponding Mauchly's test of sphericity and Greenhouse-Geisser correction. Unpaired data were analyzed with one-way ANOVA. Tukey or Dunnett multiple-comparisons adjustments were conducted only if the ANOVA F value was significant. P values of < 0.05 (indicated *) were considered significant. The Tukey test was used to compare every mean with every other mean. The Dunnett test was used to assess differences from the control (application of PSS or DMSO as a vehicle control). SigmaPlot 12.5 (RRID:SCR_003210) or OriginPro 9.0 (RRID:SCR_014212) software was used to perform statistical tests.

2.9 | Nomenclature of targets and ligands

Key protein targets and ligands in this article are hyperlinked to corresponding entries in http://www.guidetopharmacology.org, and are permanently archived in the Concise Guide to PHARMACOLOGY 2021/22 (Alexander et al., 2021).

3 | RESULTS

3.1 | Effect of the antidepressant drugs fluoxetine and amitriptyline on $K_{ir}4.1$ and $K_{ir}4.1/K_{ir}5.1$ channels

It was previously reported that the serotonin reuptake blocker fluoxetine effectively inhibits $K_{ir}4.1$ channel activity in heterologous expression cell systems (Furutani et al., 2009; Kharade et al., 2018; Ohno et al., 2007). Our studies in CHO cells overexpressing $K_{ir}4.1$ or both $K_{ir}4.1$ and $K_{ir}5.1$ subunits confirmed that the application of 100 μM fluoxetine suppresses homomeric $K_{ir}4.1$ single-channel activity (Figure 1a) but does not affect $K_{ir}4.1/K_{ir}5.1$ (Figure 1b). It is well established that $K_{ir}4.1/K_{ir}5.1$ is a major basolateral channel in distal and collecting duct principal cells which has a higher single-channel conductance relative to $K_{ir}4.1$ homomers, as confirmed by current-voltage relations shown in Figure 1 (21 ± 2 vs 37 ± 2 pS, for homo- and hetereomeric channels correspondingly). Our recent data also revealed that tricyclic antidepressant (TCA) amitriptyline, but not fluoxetine, drastically decreases the macroscopic K^+-selective conductance in CCD principal cells (Zaika et al., 2016). Here we demonstrated that the application of amitriptyline (100 μM) in CHO cells overexpressing $K_{ir}4.1$ and $K_{ir}5.1$ subunits produces up to a 51% decrease in $K_{ir}4.1/K_{ir}5.1$ single-channel activity (NP_o) (Figure 1b). However, contradictory to previous reports (Kharade et al., 2018; Su et al., 2007), amitriptyline did not affect the homomeric $K_{ir}4.1$ channel (Figure 1a).

3.2 | Inhibition of $K_{ir}4.1/K_{ir}5.1$ but not $K_{ir}4.1$ channel affects epithelial Na^+ transport in cultured $mCCD_{cl1}$ cells

Next, we examined whether inhibition of $K_{ir}4.1$ or $K_{ir}4.1/K_{ir}5.1$ channels would affect apical Na^+ transport in polarized $mCCD_{cl1}$ epithelia. The expression of both $K_{ir}4.1$ and $K_{ir}5.1$ subunits in $mCCD_{cl1}$ cell line was confirmed by immunohistochemical studies (Figure S1). Figure 2a represents the effect of the basolateral application of fluoxetine or amitriptyline on equivalent short-circuit current (I_{eq}) measured in polarized epithelial $mCCD_{cl1}$ cells at different time points. We show that the application of 100 μM fluoxetine does not affect I_{eq} up to 2 hrs after the treatment. However, 50 μM amitriptyline significantly decreases I_{eq} after application in all time points of the protocol. Importantly, amitriptyline produces a similar effect on I_{eq} when applied either to the basolateral or apical side of the epithelia (Figure 2b). Amitriptyline is a highly lipophilic molecule (Gupta et al., 1999), and like other TCA is characterized by rapid permeabilization due to affinity for cell membranes, enabling access to K^+ channel from the cytosol. The suppressive effect of amitriptyline on I_{eq} was dose-dependent with an IC_{50} of 15.0 μM (Figure 2c). To eliminate the possibility that the suppressive effect of amitriptyline on I_{eq} may be related to the inhibition of ROMK channels, we conducted studies with a specific blocker of ROMK, VU591 (Fodstad et al., 2009; Kharade et al., 2018). Our data demonstrates that the apical application of 1 μM VU591 does not affect the amiloride-sensitive I_{eq} in polarized $mCCD_{cl1}$ epithelia (Figure S2). We further supported our observation that basolateral K^+ conductance can modulate Na^+ transport using a recently developed K_{ir} channel blocker, VU0134992 (VU992) (Kharade et al., 2018). It was shown that this inhibitor is 9-fold more selective for homomeric $K_{ir}4.1$ (IC_{50} value of 0.97 μM) over heteromeric $K_{ir}4.1/K_{ir}5.1$ (IC_{50} = 9 μM) channels. Figure 2d shows that basolateral application of VU992 in concentrations

specific for $K_{ir}4.1$ (3 μM) has no effect on I_{eq}. However, higher concentrations of VU992 (30 and 300 μM) which are able to block both homo and heteromeric channels, significantly reduced Na^+ transport in polarized epithelia. The effect of high VU992 concentrations was similar to amitriptyline (Figures 2e). Furthermore, we confirmed these observations by analyzing the effect of amitriptyline and high concentrations of VU992 on ENaC activity in $mCCD_{cl1}$ cells. Figure 3 shows that acute application of either amitriptyline or 30 μM VU992 significantly reduces ENaC single-channel activity. The amplitude of single ENaC current was not affected neither after amitriptyline or VU992 application (0.59 ± 0.08 vs. 0.54 ± 0.07 (n = 7) and 0.82 ± 0.05 vs. 0.65 ± 0.06 (n = 6), pA for control vs. amitriptyline or VU992-treated, correspondingly). Moreover, preincubation of $mCCD_{cl1}$ cells in amitriptyline for more than 2 hrs resulted in decreased ENaC activity (NP_o control: 1.03 ± 0.20 (n=28) vs amitriptyline-treated 0.11 ± 0.04 (n=8), paired sample t-test *P < 0.05). To address the possibility that amitriptyline affects Na^+ transport by direct inhibition of ENaC, we examined the effect of 100 μM amitriptyline or 30 μM VU992 on the single-channel activity of ENaC overexpressed in CHO cells. Our data demonstrates that both drugs did not affect ENaC activity (Figure S3).

3.3 Inhibition of $K_{ir}4.1/K_{ir}5.1$ channel induced cellular membrane depolarization and intracellular Ca^{2+} transient in cultured $mCCD_{cl1}$ cells.

It is well established that basolateral K_{ir} channels are involved in the maintenance of a negative resting membrane potential in epithelial cells (Zaika et al., 2016). To evaluate whether inhibition of $K_{ir}4.1/K_{ir}5.1$ channel will affect epithelial cell membrane potential, cultured $mCCD_{cl1}$ cells were loaded with voltage-sensitive fluorescent probe FluoVolt™, which increases its emission upon membrane depolarization. Figures 4a and 4b show that application either 100 μM amitriptyline or 30 μM VU992 induced substantial depolarization of membrane potential in these cells. We also examined the effect of different inhibitors of K_{ir} channels on intracellular Ca^{2+} transient in cultured $mCCD_{cl1}$ cells loaded with Fluo8 AM dye. We observed the fast and substantial increase in Fluo8 AM fluorescence intensity following the application of 30 μM VU992, which accounts for the elevation of the intracellular Ca^{2+} concentration (Figure 4c). Summary data reveal that the application of 100 μM amitriptyline or 30 μM VU992 produces a significant increase of intracellular Ca^{2+} level in $mCCD_{cl1}$ cells. Application of 100 μM fluoxetine or 3 μM VU992 did not affect Ca^{2+} transient (Figure 4d).

3.4 | Inhibition of basolateral $K_{ir}4.1/K_{ir}5.1$ channel suppresses ENaC activity in principal cells of freshly isolated CCD from both human and rodent kidneys

$K_{ir}4.1/K_{ir}5.1$ channels are highly expressed in the basolateral membranes of the distal convoluted tubule (DCT) and CCD principal cells and are essential contributors to potassium transport in the distal nephron. The inhibition of $K_{ir}4.1/K_{ir}5.1$ single-channel activity by amitriptyline in the principal cells of freshly isolated CCD from Dahl SS rats is shown in Figure 5a. Using a split-open configuration, we performed patch-clamp recordings on the apical side of principal cells (microphotograph Figure 5b) and directly detected changes in ENaC activity during the modulation of basolateral K^+ conductance in freshly isolated CCDs. Figure 5b demonstrates the significant decrease of ENaC activity after adding amitriptyline to the bath solution. The application of amitriptyline leads to a significant

reduction of $K_{ir}4.1/K_{ir}5.1$ channel amplitude but does not modulate the amplitude of ENaC (1.89 ± 0.21 vs. 1.14 ± 0.26 (n = 8), paired sample t-test $*P < 0.05$ and 0.70 ±0.10 vs. 0.66 ± 0.11 (n = 9) pA for $K_{ir}4.1/K_{ir}5.1$ and ENaC correspondingly; data are shown for control vs. amitriptyline-treated tubules).

In order to further extend this line of investigation and the feasibility of clinical use, we used freshly isolated tubules from human kidneys to interrogate $K_{ir}4.1/K_{ir}5.1$-based control of sodium transport in the collecting duct. Figure 6a represents a microphotograph of split-open (apical) and basolateral electrophysiological configurations to measure single-channel activity in human principal cells of the CCD. As shown in Figure 6b, application of amitriptyline and VU992 resulted in the inhibition of human $K_{ir}4.1/K_{ir}5.1$ single-channel activity (average amplitude of 1.82 ± 0.29 pA in control, 1.48 ± 0.12 pA after 5 min treatment with 100 μM amitriptyline, and 0.88 ± 0.06 pA after subsequent VU992 application at holding potential −60 mV). Figure 6c represents the effect of $K_{ir}4.1/K_{ir}5.1$ channel inhibition on ENaC-mediated Na^+ transport. These electrophysiological recordings represent the first pharmacological analysis of ENaC single-channel activity in a human kidney. Summary data pulled from four recordings of ENaC single-channel activity in CCDs show that the application of 100 μM amitriptyline produces a substantial decrease in ENaC NP_o but does not affect its unitary current amplitude (0.51 ± 0.09 vs. 0.47 ± 0.09 pA, control vs. amitriptyline correspondingly). The application of VU992 produced a similar effect on ENaC activity. Despite the low number of samples and exploratory analyses of the human data set, the observed behavior is consistent with our experiments in polarized epithelia and rat isolated tubules.

3.5 | Effect of pharmacological inhibition of $K_{ir}4.1/K_{ir}5.1$ channel by amitriptyline on K^+ and Na^+ homeostasis in SS rats

As was previously described in the Dahl SS rats with the functional knockout of *Kcnj16* ($SS^{Kcnj16-/-}$), the deletion of $K_{ir}4.1/K_{ir}5.1$ channels is characterized by elevated excretion of electrolytes, hypokalemia, increased expression of sodium transporters in the ASDN (ENaC, NCC, and NKCC, including active phosphorylated forms), and normal blood sodium levels (Palygin et al., 2017). To evaluate the pharmacological effect of amitriptyline on $K_{ir}4.1/K_{ir}5.1$ channel activity in an animal model to compare with published data in the knockout, we used 10–12-week-old SS rats injected three consecutive days with amitriptyline. The analyses of blood electrolytes shown in Figure 7a demonstrate that amitriptyline administration led to a significant drop in plasma K^+ (4.2 ± 0.1 vs. 3.4 ± 0.1 mmol l^{-1}, control vs. injection day 3) but did not affect plasma Na^+ levels after three days of injection. Moreover, both K^+ and Na^+ excretion was increased (Figure 7b). This increase in urinary electrolytes was accompanied by elevated diuresis (Figure 7c), but we did not detect significant creatinine clearance changes (108.2 ± 11.5 vs. 119.4 ± 11.4 ml h^{-1}, control vs. injection day 3 correspondingly). These data indicate that pharmacological inhibition of $K_{ir}4.1/K_{ir}5.1$ channel may directly modulate potassium homeostasis, diuresis, and sodium excretion. Figure 8 demonstrates the upregulation of both the total and phosphorylated (active) forms of NCC in renal cortical tissue of rats treated for three days with amitriptyline compared to control. These data are consistent with findings in the $SS^{Kcnj16-/-}$ rat, which indicate that the blockade of $K_{ir}4.1/K_{ir}5.1$ channel produces a salt-wasting phenotype

despite the increased compensatory levels of the NCC transporter in ADSN (Palygin et al., 2017). The Western blots show an increase in ENaC α-subunit expression, without any changes in cleaved and noncleaved forms of γ-ENaC (Figure 8), similar to the reported γ-ENaC expression for the collecting duct system-specific $K_{ir}4.1$ knockout mouse (Penton et al., 2020).

4 | DISCUSSION

The key findings of the present study are: 1) inhibition of $K_{ir}4.1/K_{ir}5.1$, but not a $K_{ir}4.1$ channels decrease ENaC activity; these effects are most likely mediated by induced depolarization of membrane potential and increase in intracellular Ca^{2+} level; 2) acute inhibition of inwardly rectifying K^+ channel conductance by amitriptyline or high concentrations of VU992 promotes the decrease in ENaC activity in principal cells in rat and human CCD; 3) *in vivo* amitriptyline treatment recapitulates the effect of $K_{ir}5.1$ deletion in SS rats on electrolyte homeostasis and expression of total and phosphorylated NCC in the distal nephron.

Although the essential role of $K_{ir}4.1$-composed K^+ channels for the regulation of K^+ handling and electrolyte homeostasis in the kidney is well established in knockout rodent models (Manis et al., 2019; Penton et al., 2020; Su et al., 2016), the exact physiological mechanisms as well as the role of ENaC, BK-channels, Ca^{2+} entry, or Mg^{2+} transport in this processes still require further investigation. The difference between models with deletion of $K_{ir}4.1$ or $K_{ir}5.1$ subunit should be noted. Deletion of $K_{ir}4.1$ eliminates the activity of both channels, downregulates NCC expression, and induces alkalosis (Scholl et al., 2009). In contrast, deletion of $K_{ir}5.1$ removes only heteromeric $K_{ir}4.1/K_{ir}5.1$ channels, upregulates $K_{ir}4.1$ and NCC expression (Palygin et al., 2017), induces metabolic acidosis (Paulais et al., 2011; Puissant et al., 2019), triggers hyperactivity of the RAAS system and preserves the ability to regulate basolateral K^+ transport and survivability on a high K^+ diet (Manis et al., 2019). On the other hand, deletion of both subunits is characterized by severe hypokalemia and upregulation of ENaC expression in the kidney (Manis et al., 2019; Wu et al., 2020a). Pharmacological inhibition of the channels could result in different outcomes compared to knockout animal studies. For example, it was reported that inhibition of NCC transport activity by pharmacological means does not increase Na^+ reabsorption through ENaC (Hunter et al., 2014). Here we used available pharmacological tools to exclude the discrepancy of the different genetic models and establish the primary basolateral $K_{ir}4.1/K_{ir}5.1$ channel's (Wu et al., 2020b) role in regulating ENaC in CCD.

Studies in heterologous expression systems reported that antidepressant TCA drugs act as reversible blockers of $K_{ir}4.1$ channels (Furutani et al., 2009; Ohno et al., 2007). Our data shows that 100 μM fluoxetine effectively inhibits single-channel $K_{ir}4.1$ activity but does not affect heteromeric channel activity in CHO cells. Amitriptyline (100 μM) displays an acute inhibitory effect on $K_{ir}4.1/K_{ir}5.1$ current but has no effect on $K_{ir}4.1$. Interestingly, in previous studies, the inhibitory effect of amitriptyline on $K_{ir}4.1$ was demonstrated using patch-clamp studies and thallium (Tl^+) flux assay (Kharade et al., 2018; Su et al., 2007). It was shown that the inhibitory action of tricyclic antidepressants on K_{ir} channels is dependent on extracellular concentrations of K^+ with a more robust effect in the conditions of smaller

potassium gradient. So, we suggest that in our configuration (with 150 mM of K^+ in pipette solution), the inhibitory effect of amitriptyline on both homomeric and heteromeric channels maybe be blunted. In our *ex vivo* study, amitriptyline induced a significant suppression of NP_o as well as a decrease in unitary $K_{ir}4.1/K_{ir}5.1$ current amplitude recorded from rat principal CCD cells, indicating that inhibition of this basolateral channel will result in membrane depolarization. Our data with membrane voltage dye FluoVolt™ in cultured epithelial $mCCD_{cl1}$ cells supports this assumption. Similar inhibitory effects of amitriptyline or high concentrations of VU992 were observed in human CCD principal cells. Our data demonstrating the important role of basolateral K^+ conductance in the regulation of membrane potential support previous findinds on mice *Kcnj10* knockout model and C57BL/6J mice (Zaika et al., 2016; Zhang et al., 2014). Taken together, our studies demonstrate that amitriptyline predominantly affects $K_{ir}4.1/K_{ir}5.1$ channel rather than homomeric $K_{ir}4.1$ channel activity and could be a valuable pharmacological tool to better understand the physiological role of these channels.

Using an electrophysiological approach, we show that acute application of amitriptyline and VU992 in concentrations that produce an inhibitory effect on heteromeric $K_{ir}4.1/K_{ir}5.1$ channel results in substantial suppression of the I_{eq} measured in polarized epithelial $mCCD_{cl1}$ cells. The inhibition of basolateral K^+ conductance reduces single-channel ENaC channel activity in $mCCD_{cl1}$ and principal cells of freshly isolated rodent and human CCD tubules. The reduction of ENaC activity is not attributed to the direct effect of amitriptyline or VU992 since they do not cause any change in Na^+ conductance in CHO cells overexpressing ENaC (Figure S3). Also, the suppressive effect of amitriptyline on amiloride-sensitive I_{eq} is not likely related to unspecific inhibition of ROMK, since ROMK blockade by VU591 does not affect amiloride-sensitive I_{eq} in polarized epithelial cortical collecting principal $mCCD_{cl1}$ cells (Figure S2). These data is in agreement with the previous *in vivo* study with ROMK inhibitor and benzamil, suggesting that ROMK inhibition does not abolish ENaC-mediated Na^+ transport in the collecting duct (Kharade et al., 2016). Interestingly, neither fluoxetine nor VU992 at concentrations specific for $K_{ir}4.1$ channel affected ENaC activity measured with I_{eq}. This implies that the homomeric $K_{ir}4.1$ channel likely plays only a minor role in controlling apical Na^+ transport in CCD.

Our study shows that acute inhibition of $K_{ir}4.1/K_{ir}5.1$ channel induced membrane depolarization, supporting the established role of these channels in the control of membrane potential (Zaika et al., 2016; Zhang et al., 2014). Indeed, classic physiology studies indicate the direct relationship between the activity of Na^+/K^+ ATPase and potassium conductance on the basolateral membrane (Kubota et al., 1983; Lapointe et al., 1990; Matsumura et al., 1984). We also show that pharmacological inhibition of $K_{ir}4.1/K_{ir}5.1$ channel promotes the increase in intracellular Ca^{2+} concentration (Figure 4). Although the exact mechanism involved in the regulation of intracellular Ca^{2+} by the block of basolateral K_{ir} channel activity needs further in-depth investigation, the inhibitory effect of intracellular Ca^{2+} increase on ENaC activity is well documented (Gu, 2008; Ishikawa et al., 1998; Ismailov et al., 1997; Palmer & Frindt, 1987). It was proposed that Ca^{2+} could act directly on the channel pore or through activation of intracellular secondary messengers such as calmodulin, protein kinase C and prostaglandin (Gu, 2008; Palmer & Frindt, 1987). We suggest that the reduction of electrochemical gradient triggered by the depolarization of the

basolateral membrane and/or the increase in intracellular Ca^{2+} could explain the modulatory effect of $K_{ir}4.1/K_{ir}5.1$ inhibition on ENaC activity. In agreement with this statement, a recent electrophysiological study in mice indicates that the deletion of $K_{ir}5.1$ decreased ENaC currents in the late distal convoluted tubule, and this effect is even more prominent under high salt conditions (Duan et al., 2021). Furthermore, the increase in intracellular Ca^{2+} level in response to inhibition of basolateral K^+ conductance could also mediate kaliuresis observed in rats exposed to amitriptyline. In this condition, a large conductance, voltage- and Ca^{2+}-gated K^+ BK channel presented along the apical side of the distal nephron become activated and may be primarily responsible for renal K^+ excretion.

A common side effect of amitriptyline overdose is orthostatic hypotension, metabolic acidosis, hypokalemia (Glassman & Preud'homme, 1993; Kerr et al., 2001; Scalco et al., 2000), which surprisingly mimics phenotypic features of $SS^{Kcnj16-/-}$ rats. Although the effect of downregulation of basolateral K^+ conductance on blood pressure and salt-wasting phenotypes can vary across models, hypokalemia is always a distinctive feature of this pathological condition. This emphasizes the central role of K_{ir} channels to control plasma K^+ levels. In our *in vivo* study, i.p. injections of amitriptyline for a few days significantly shifted blood potassium concentrations towards hypokalemic values. The SS rats also exhibited elevated K^+ and Na^+ excretion. The Western blots shows an increase in αENaC expression but no changes in γENaC or it cleaved form by amitriptyline treatment (Figure 8). We also observed a substantial increase in the expression of total and phosphorylated forms of NCC. Likewise, the stimulation of DCT function and increased NCC expression was previously reported in rat and mice models with knockout of *Kcnj16* (Palygin et al., 2017; Paulais et al., 2011). These data allow us to presume that amitriptyline treatment in Dahl SS rats recapitulates the renal phenotype developed after genetic ablation of *Kcnj16*, but not *Kcnj10* knockout. In the future, the development of highly specific Kir4.1/Kir5.1 pharmacological tools will allow us to explore in more detail the ways in which basolateral K^+ conductance contributes to the regulation of Na^+ transport in the kidney.

In summary, our study demonstrates the essential role of renal $K_{ir}4.1/K_{ir}5.1$ channel not only in the control of plasma K^+ but also on the regulation of ENaC-mediated sodium reabsorption. Therefore, future studies are critical to elucidate the physiological effects of $K_{ir}4.1/K_{ir}5.1$ inhibition *in vivo* in this and other models, to more fully define the mechanistic actions and potential for therapeutic use.

Supplementary Material

Refer to Web version on PubMed Central for supplementary material.

Acknowledgments:

This research was supported by the National Institutes of Health grants R56 DK121750 and R01 DK126720 (to OP), R35 HL135749 (to ASt), R01 DK120821 (to JSD and ASt), T32 HL134643 CVC A.O. Smith Fellowship (to CAK), Department of Veteran Affairs grant I01 BX004024 (to ASt), endowed funds from the SC SmartState Centers of Excellence (to OP), and RSF №19-14-00114 (to ASh). The authors would like to acknowledge Ashraf El-Meanawy (Department of Nephrology, MCW) for work with human tissues and Nicholas J. Burgraff for help with *in vivo* animal studies.

Declaration of transparency and scientific rigour:

This Declaration acknowledges that this paper adheres to the principles for transparent reporting and scientific rigour of preclinical research as stated in the BJP guidelines for Natural Products Research, Design and Analysis, Immunoblotting and Immunochemistry, and Animal Experimentation, and as recommended by funding agencies, publishers and other organisations engaged with supporting research.

Data availability:

The data that support the findings of this study are available from the corresponding author upon reasonable request.

ABBREVIATIONS:

ASDN	aldosterone-sensitive distal nephron
CCD	cortical collecting duct
CD	collecting ducts
CHO	Chinese hamster ovary
CNS	central nervous system
CNT	connecting tubule
DCT	distal convoluted tubule
ENaC	epithelial Na^+ channel
HCTZ	hydrochlorothiazide
I_{eq}	equivalent short-circuit current
K_{ir}	inwardly rectifying K^+
ROMK	renal outer medullary potassium channel ($K_{ir}1.1$)
NCC	thiazide-sensitive Na^+-Cl^- cotransporter
TCA	tricyclic antidepressant
RAAS	renin-angiotensin-aldosterone system

REFERENCES

Alexander SP, Mathie A, Peters JA, Veale EL, Striessnig J, Kelly E, et al. (2021). THE CONCISE GUIDE TO PHARMACOLOGY 2021/22: Ion channels. Br J Pharmacol 178 Suppl 1: S157–S245. [PubMed: 34529831]

Alexander SPH, Roberts RE, Broughton BRS, Sobey CG, George CH, Stanford SC, et al. (2018). Goals and practicalities of immunoblotting and immunohistochemistry: A guide for submission to the British Journal of Pharmacology. Br J Pharmacol 175: 407–411. [PubMed: 29350411]

Assmus AM, Mansley MK, Mullins LJ, Peter A, & Mullins JJ (2018). mCCDcl1 cells show plasticity consistent with the ability to transition between principal and intercalated cells. Am J Physiol Renal Physiol 314: F820–F831. [PubMed: 29357433]

Bockenhauer D, Feather S, Stanescu HC, Bandulik S, Zdebik AA, Reichold M, et al. (2009). Epilepsy, ataxia, sensorineural deafness, tubulopathy, and KCNJ10 mutations. The New England journal of medicine 360: 1960–1970. [PubMed: 19420365]

Cuevas CA, Su XT, Wang MX, Terker AS, Lin DH, McCormick JA, et al. (2017). Potassium Sensing by Renal Distal Tubules Requires Kir4.1. J Am Soc Nephrol 28: 1814–1825. [PubMed: 28052988]

Curtis MJ, Alexander S, Cirino G, Docherty JR, George CH, Giembycz MA, et al. (2018). Experimental design and analysis and their reporting II: updated and simplified guidance for authors and peer reviewers. Br J Pharmacol 175: 987–993. [PubMed: 29520785]

Curtis MJ, Bond RA, Spina D, Ahluwalia A, Alexander SP, Giembycz MA, et al. (2015). Experimental design and analysis and their reporting: new guidance for publication in BJP. Br J Pharmacol 172: 3461–3471. [PubMed: 26114403]

Dahl LK, Leitl G, & Heine M (1972). Influence of dietary potassium and sodium/potassium molar ratios on the development of salt hypertension. J Exp Med 136: 318–330. [PubMed: 5043414]

Duan XP, Wu P, Zhang DD, Gao ZX, Xiao Y, Ray EC, et al. (2021). Deletion of Kir5.1 abolishes the effect of high Na(+) intake on Kir4.1 and Na(+)-Cl(-) cotransporter. Am J Physiol Renal Physiol 320: F1045–F1058. [PubMed: 33900854]

Fodstad H, Gonzalez-Rodriguez E, Bron S, Gaeggeler H, Guisan B, Rossier BC, et al. (2009). Effects of mineralocorticoid and K+ concentration on K+ secretion and ROMK channel expression in a mouse cortical collecting duct cell line. Am J Physiol Renal Physiol 296: F966–975. [PubMed: 19297448]

Furutani K, Ohno Y, Inanobe A, Hibino H, & Kurachi Y (2009). Mutational and in silico analyses for antidepressant block of astroglial inward-rectifier Kir4.1 channel. Mol Pharmacol 75: 1287–1295. [PubMed: 19264848]

Gaeggeler HP, Gonzalez-Rodriguez E, Jaeger NF, Loffing-Cueni D, Norregaard R, Loffing J, et al. (2005). Mineralocorticoid versus glucocorticoid receptor occupancy mediating aldosterone-stimulated sodium transport in a novel renal cell line. J Am Soc Nephrol 16: 878–891. [PubMed: 15743993]

Glassman AH, & Preud'homme XA (1993). Review of the cardiovascular effects of heterocyclic antidepressants. J Clin Psychiatry 54 Suppl: 16–22.

Golosova D, Palygin O, Bohovyk R, Klemens CA, Levchenko V, Spires DR, et al. (2020). Role of opioid signaling in kidney damage during the development of salt-induced hypertension. Life Sci Alliance 3.

Gu Y (2008). Effects of [Ca2+]i and pH on epithelial Na+ channel activity of cultured mouse cortical collecting ducts. J Exp Biol 211: 3167–3173. [PubMed: 18805816]

Gupta SK, Shah JC, & Hwang SS (1999). Pharmacokinetic and pharmacodynamic characterization of OROS and immediate-release amitriptyline. Br J Clin Pharmacol 48: 71–78. [PubMed: 10383563]

Hunter RW, Craigie E, Homer NZ, Mullins JJ, & Bailey MA (2014). Acute inhibition of NCC does not activate distal electrogenic Na+ reabsorption or kaliuresis. Am J Physiol Renal Physiol 306: F457–467. [PubMed: 24402096]

Isaeva E, Fedoriuk M, Bohovyk R, Klemens CA, Khedr S, Golosova D, et al. (2019). Vibrodissociation method for isolation of defined nephron segments from human and rodent kidneys. Am J Physiol Renal Physiol 317: F1398–F1403. [PubMed: 31588797]

Ishikawa T, Marunaka Y, & Rotin D (1998). Electrophysiological characterization of the rat epithelial Na+ channel (rENaC) expressed in MDCK cells. Effects of Na+ and Ca2+. J Gen Physiol 111: 825–846. [PubMed: 9607939]

Ismailov II, Berdiev BK, Shlyonsky VG, & Benos DJ (1997). Mechanosensitivity of an epithelial Na+ channel in planar lipid bilayers: release from Ca2+ block. Biophys J 72: 1182–1192. [PubMed: 9138565]

Kerr GW, McGuffie AC, & Wilkie S (2001). Tricyclic antidepressant overdose: a review. Emerg Med J 18: 236–241. [PubMed: 11435353]

Kharade SV, Flores D, Lindsley CW, Satlin LM, & Denton JS (2016). ROMK inhibitor actions in the nephron probed with diuretics. Am J Physiol Renal Physiol 310: F732–F737. [PubMed: 26661652]

Kharade SV, Kurata H, Bender AM, Blobaum AL, Figueroa EE, Duran A, et al. (2018). Discovery, Characterization, and Effects on Renal Fluid and Electrolyte Excretion of the Kir4.1 Potassium Channel Pore Blocker, VU0134992. Mol Pharmacol 94: 926–937. [PubMed: 29895592]

Khedr S, Palygin O, Pavlov TS, Blass G, Levchenko V, Alsheikh A, et al. (2019). Increased ENaC activity during kidney preservation in Wisconsin solution. BMC Nephrol 20: 145. [PubMed: 31035971]

Kubota T, Biagi BA, & Giebisch G (1983). Intracellular potassium activity measurements in single proximal tubules of Necturus kidney. J Membr Biol 73: 51–60. [PubMed: 6864767]

Lapointe JY, Garneau L, Bell PD, & Cardinal J (1990). Membrane crosstalk in the mammalian proximal tubule during alterations in transepithelial sodium transport. Am J Physiol 258: F339–345. [PubMed: 2309892]

Lilley E, Stanford SC, Kendall DE, Alexander SPH, Cirino G, Docherty JR, et al. (2020). ARRIVE 2.0 and the British Journal of Pharmacology: Updated guidance for 2020. Br J Pharmacol 177: 3611–3616. [PubMed: 32662875]

Manis AD, Palygin O, Isaeva E, Levchenko V, LaViolette PS, Pavlov TS, et al. (2021). Kcnj16 knockout produces audiogenic seizures in the Dahl salt-sensitive rat. JCI Insight 6.

Manis AD, Palygin O, Khedr S, Levchenko V, Hodges MR, & Staruschenko A (2019). Relationship between the renin-angiotensin-aldosterone system and renal Kir5.1 channels. Clin Sci (Lond) 133: 2449–2461. [PubMed: 31799617]

Matsumura Y, Cohen B, Guggino WB, & Giebisch G (1984). Electrical effects of potassium and bicarbonate on proximal tubule cells of Necturus. J Membr Biol 79: 145–152. [PubMed: 6748054]

McGrath JC, & Lilley E (2015). Implementing guidelines on reporting research using animals (ARRIVE etc.): new requirements for publication in BJP. Br J Pharmacol 172: 3189–3193. [PubMed: 25964986]

Mente A, O'Donnell MJ, Rangarajan S, McQueen MJ, Poirier P, Wielgosz A, et al. (2014). Association of urinary sodium and potassium excretion with blood pressure. The New England journal of medicine 371: 601–611. [PubMed: 25119606]

Mukherjee A, Wang Z, Kinlough CL, Poland PA, Marciszyn AL, Montalbetti N, et al. (2017). Specific Palmitoyltransferases Associate with and Activate the Epithelial Sodium Channel. J Biol Chem 292: 4152–4163. [PubMed: 28154191]

Ohno Y, Hibino H, Lossin C, Inanobe A, & Kurachi Y (2007). Inhibition of astroglial Kir4.1 channels by selective serotonin reuptake inhibitors. Brain Res 1178: 44–51. [PubMed: 17920044]

Palmer LG, & Frindt G (1987). Effects of cell Ca and pH on Na channels from rat cortical collecting tubule. Am J Physiol 253: F333–339. [PubMed: 2441611]

Palygin O, Levchenko V, Ilatovskaya DV, Pavlov TS, Pochynyuk OM, Jacob HJ, et al. (2017). Essential role of K_{ir}5.1 channels in renal salt handling and blood pressure control. JCI Insight 2: e92331.

Paulais M, Bloch-Faure M, Picard N, Jacques T, Ramakrishnan SK, Keck M, et al. (2011). Renal phenotype in mice lacking the Kir5.1 (Kcnj16) K+ channel subunit contrasts with that observed in SeSAME/EAST syndrome. Proceedings of the National Academy of Sciences of the United States of America 108: 10361–10366. [PubMed: 21633011]

Pavlov TS, Levchenko V, & Staruschenko A (2014). Role of Rho GDP dissociation inhibitor alpha in control of epithelial sodium channel (ENaC)-mediated sodium reabsorption. J Biol Chem 289: 28651–28659. [PubMed: 25164814]

Penton D, Vohra T, Banki E, Wengi A, Weigert M, Forst AL, et al. (2020). Collecting system-specific deletion of Kcnj10 predisposes for thiazide- and low-potassium diet-induced hypokalemia. Kidney Int 97: 1208–1218. [PubMed: 32299681]

Puissant MM, Muere C, Levchenko V, Manis AD, Martino P, Forster HV, et al. (2019). Genetic mutation of Kcnj16 identifies Kir5.1-containing channels as key regulators of acute and chronic pH homeostasis. FASEB J 33: 5067–5075. [PubMed: 30605394]

Reichold M, Zdebik AA, Lieberer E, Rapedius M, Schmidt K, Bandulik S, et al. (2010). KCNJ10 gene mutations causing EAST syndrome (epilepsy, ataxia, sensorineural deafness, and tubulopathy) disrupt channel function. Proceedings of the National Academy of Sciences of the United States of America 107: 14490–14495. [PubMed: 20651251]

Scalco MZ, de Almeida OP, Hachul DT, Castel S, Serro-Azul J, & Wajngarten M (2000). Comparison of risk of orthostatic hypotension in elderly depressed hypertensive women treated with nortriptyline and thiazides versus elderly depressed normotensive women treated with nortriptyline. Am J Cardiol 85: 1156–1158, A1159. [PubMed: 10781773]

Schlingmann KP, Renigunta A, Hoorn EJ, Forst AL, Renigunta V, Atanasov V, et al. (2021). Defects in KCNJ16 Cause a Novel Tubulopathy with Hypokalemia, Salt Wasting, Disturbed Acid-Base Homeostasis, and Sensorineural Deafness. J Am Soc Nephrol 32: 1498–1512. [PubMed: 33811157]

Scholl UI, Choi M, Liu T, Ramaekers VT, Hausler MG, Grimmer J, et al. (2009). Seizures, sensorineural deafness, ataxia, mental retardation, and electrolyte imbalance (SeSAME syndrome) caused by mutations in KCNJ10. Proceedings of the National Academy of Sciences of the United States of America 106: 5842–5847. [PubMed: 19289823]

Staruschenko A (2018). Beneficial effects of high potassium: contribution of renal basolateral K^+ channels. Hypertension 71: 1015–1022. [PubMed: 29712740]

Staruschenko A, Pochynyuk O, & Stockand JD (2005). Regulation of epithelial Na+ channel activity by conserved serine/threonine switches within sorting signals. Journal of Biological Chemistry 280: 39161–39167. [PubMed: 16203727]

Su S, Ohno Y, Lossin C, Hibino H, Inanobe A, & Kurachi Y (2007). Inhibition of astroglial inwardly rectifying Kir4.1 channels by a tricyclic antidepressant, nortriptyline. J Pharmacol Exp Ther 320: 573–580. [PubMed: 17071817]

Su XT, Zhang C, Wang L, Gu R, Lin DH, & Wang WH (2016). Disruption of KCNJ10 (Kir4.1) stimulates the expression of ENaC in the collecting duct. Am J Physiol Renal Physiol 310: F985–993. [PubMed: 26887833]

Tobian L (1991). Salt and hypertension. Lessons from animal models that relate to human hypertension. Hypertension 17: I52–58. [PubMed: 1987012]

Virani SS, Alonso A, Benjamin EJ, Bittencourt MS, Callaway CW, Carson AP, et al. (2020). Heart Disease and Stroke Statistics-2020 Update: A Report From the American Heart Association. Circulation 141: e139–e596. [PubMed: 31992061]

Wu P, Gao ZX, Zhang DD, Duan XP, Terker AS, Lin DH, et al. (2020a). Effect of Angiotensin II on ENaC in the Distal Convoluted Tubule and in the Cortical Collecting Duct of Mineralocorticoid Receptor Deficient Mice. J Am Heart Assoc 9: e014996. [PubMed: 32208832]

Wu P, Su XT, Gao ZX, Zhang DD, Duan XP, Xiao Y, et al. (2020b). Renal Tubule Nedd4–2 Deficiency Stimulates Kir4.1/Kir5.1 and Thiazide-Sensitive NaCl Cotransporter in Distal Convoluted Tubule. J Am Soc Nephrol 31: 1226–1242. [PubMed: 32295826]

Zaika O, Palygin O, Tomilin V, Mamenko M, Staruschenko A, & Pochynyuk O (2016). Insulin and IGF-1 activate Kir4.1/5.1 channels in cortical collecting duct principal cells to control basolateral membrane voltage. Am J Physiol Renal Physiol 310: F311–321. [PubMed: 26632606]

Zhang C, Wang L, Zhang J, Su XT, Lin DH, Scholl UI, et al. (2014). KCNJ10 determines the expression of the apical Na-Cl cotransporter (NCC) in the early distal convoluted tubule (DCT1). Proceedings of the National Academy of Sciences of the United States of America 111: 11864–11869. [PubMed: 25071208]

BULLET POINT SUMMARY:

What is already known

- Inwardly rectifying K^+ (K_{ir}) channels of the distal nephron, specifically $K_{ir}4.1$ and $K_{ir}4.1/K_{ir}5.1$, play a critical role in determining blood K^+ level.

What this study adds

- Our study reveals that inhibition of $K_{ir}4.1/K_{ir}5.1$ channel, but not $K_{ir}4.1$ suppresses ENaC activity.
- Inhibition of renal $K_{ir}4.1/K_{ir}5.1$ reduces blood potassium level, promotes diuresis and natriuresis.

What is the clinical significance?

- Inhibition of $K_{ir}4.1/K_{ir}5.1$ channel affects ENaC activity and increases natriuresis, which potentially can help to lower blood pressure and reduce the risk of cardiovascular disease.
- This study identifies $K_{ir}4.1/K_{ir}5.1$ channel as a new potential therapeutic target for the control of electrolyte homeostasis and hyperkalemia.

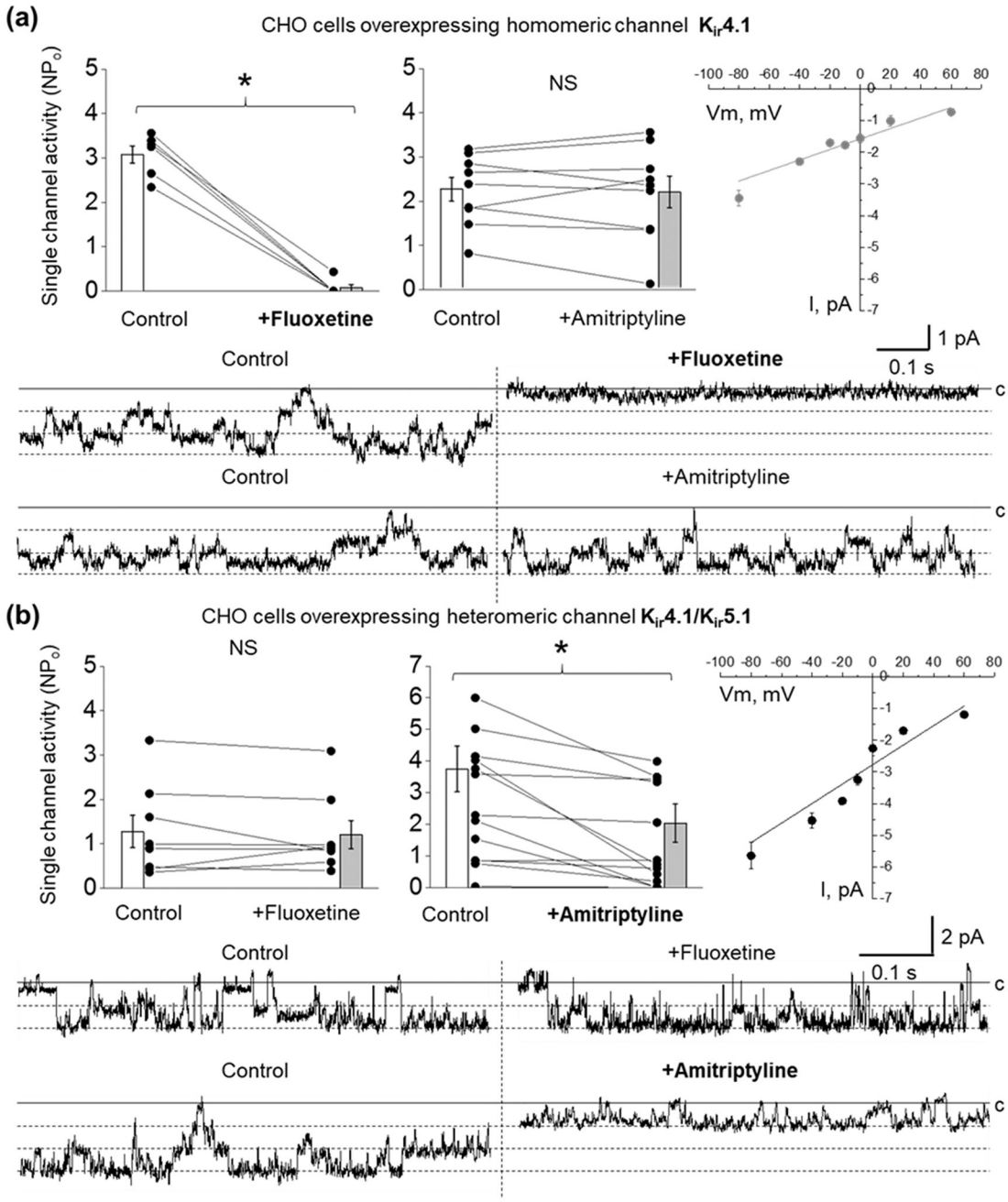

FIGURE 1.

Effect of fluoxetine and amitriptyline on $K_{ir}4.1$ and $K_{ir}4.1/K_{ir}5.1$ currents overexpressed in CHO cells. Summary graphs of homomeric $K_{ir}4.1$ (a) and heteromeric $K_{ir}4.1/K_{ir}5.1$ (b) single-channel activity (NP_o) after application of PSS as vehicle control, 100 μM fluoxetine ($K_{ir}4.1$, n = 6; $K_{ir}4.1/K_{ir}5.1$, n = 8) or 100 μM amitriptyline ($K_{ir}4.1$, n = 9; $K_{ir}4.1/K_{ir}5.1$, n =13). Paired sample t-test $*P < 0.05$. Single-channel closed (c) and open states for the representative recorded currents are indicated by solid and dashed lines. Current-voltage relationships of $K_{ir}4.1$ (n = 6) and heteromeric $K_{ir}4.1/K_{ir}5.1$ (n = 6) current are shown in the left panels (linear fitting, instrumental weight. Adj. R-Square ≥0.83).

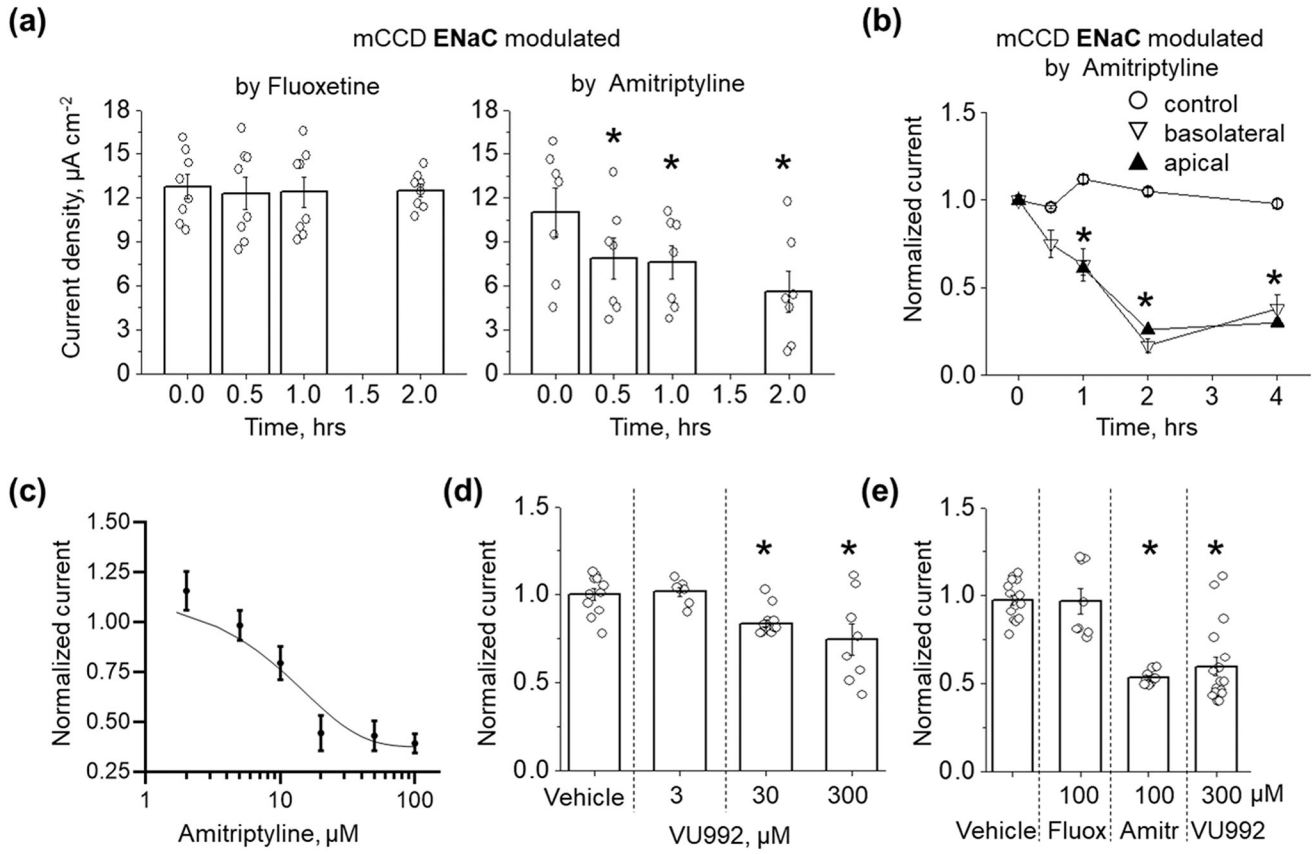

FIGURE 2.

Effect of potassium channel inhibitors on I_{eq} in $mCCD_{cl1}$ cells. (a) Effect of basolateral application of 100 μM fluoxetine (n = 8) and 50 μM amitriptyline (n = 7) on I_{eq} measured at different time points. One Way RM ANOVA with a Greenhouse-Geisser correction ($F(1.81, 10.87) = 14.03$, $P < 0.002$), post hoc test using Dunnett correction $^*P < 0.05$ compared to starting point. (b) Effect of apical or basolateral application of 50 μM amitriptyline on amiloride-sensitive Na^+ epithelial transport in $mCCD_{cl1}$ cells (n = 5 for each group, One Way ANOVA, Dunnett post-hoc test $^*P < 0.05$ compared to control). (c) Concentration-dependence of amitriptyline effect on I_{eq} (n = 6 per point). (d) Modulation of I_{eq} by different concentrations of VU992 (vehicle, n = 11; 3 μM, n = 7; 30 μM, n = 8; 300 μM, n = 8). (e) Summary graph for the ENaC current modulation (I_{eq}) by K_{ir} channels blockers (vehicle, n = 14; fluoxetine, n = 8; amitriptyline, n = 9; VU992, n = 17). I_{eq} for (d) and (e) recorded 2 hrs after drugs or vehicle application (One Way ANOVA, Dunnett post-hoc test, $^*P < 0.05$ compared to vehicle).

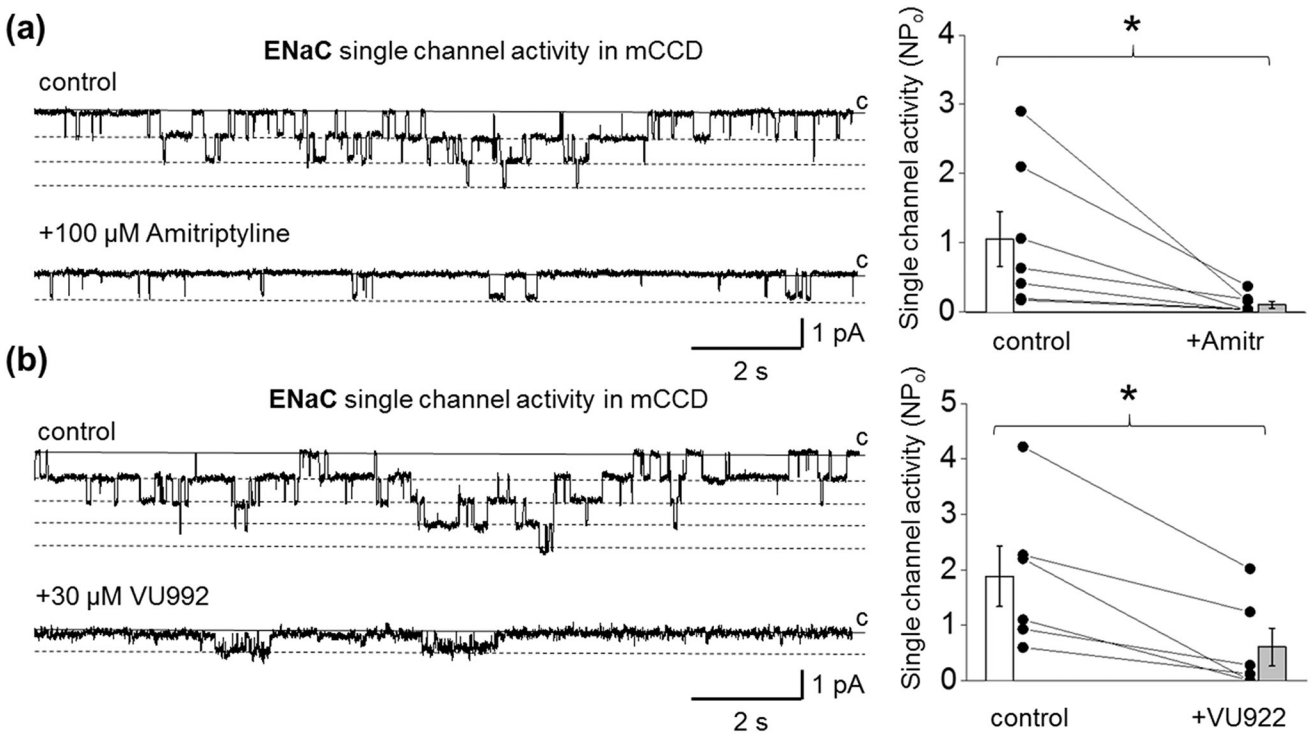

FIGURE 3.

Acute inhibition of $K_{ir}4.1/K_{ir}5.1$ channel suppresses ENaC single-channel activity in $mCCD_{cl1}$ cells. Representative traces of ENaC activity recorded in cell-attached mode after application of PSS or DMSO as vehicle control or application of 100 μM amitriptyline (a) or 30 μM VU992 (b). Conformational closed (c) and open states are indicated by solid and dashed lines. Patches were clamped to -Vp = −60 mV. Corresponding summary graphs show that application of 100 μM amitriptyline (n = 7) or 30 μM VU992 (n = 6) induced a decrease in ENaC single-channel activity. Paired sample t-test $*P < 0.05$.

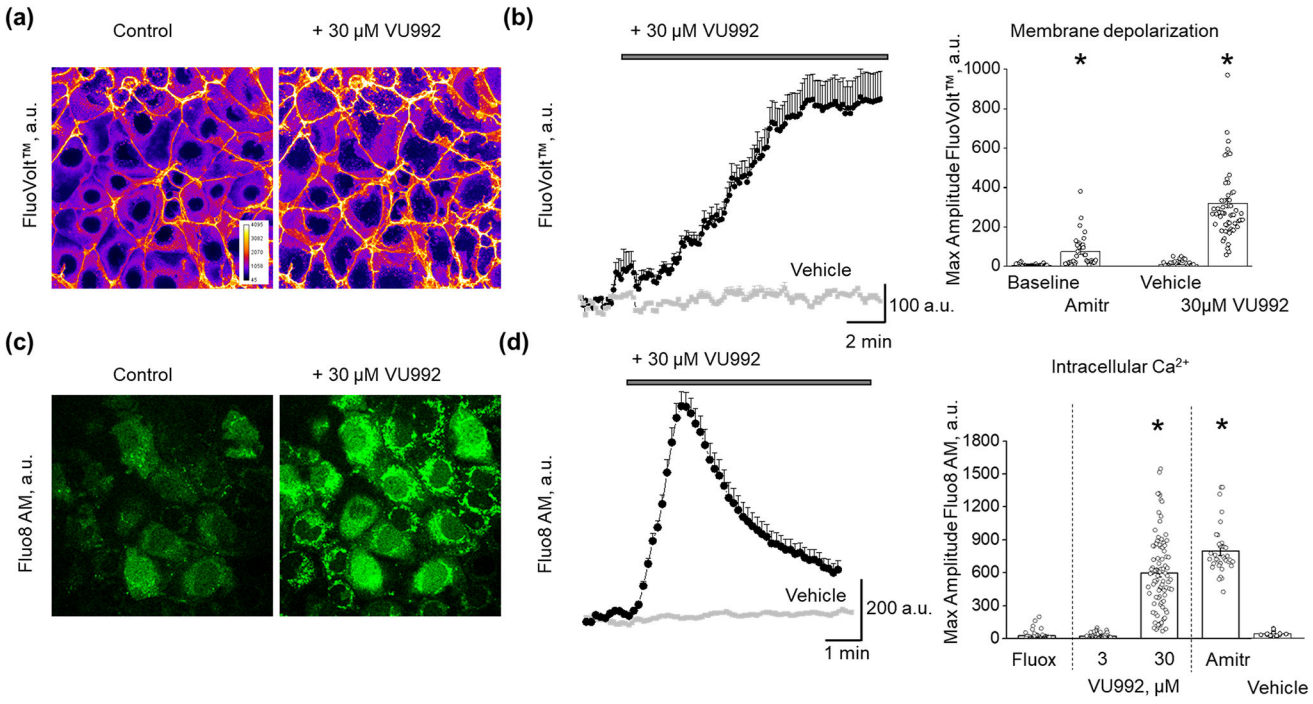

FIGURE 4.

Effect of $K_{ir}4.1$ and $K_{ir}4.1/K_{ir}5.1$ channels inhibitors on the membrane potential and intracellular Ca^{2+} concentrations in $mCCD_{cl1}$ cells. (a) Representative confocal images of $mCCD_{cl1}$ cells loaded with membrane potential dye (FluoVolt) acquired before and after application of VU992 with the corresponding graph plotting the time course of changes in the FluoVolt fluorescence intensity pooled from six cells. (b) Summary graph of the peak FluoVolt fluorescence intensity following application of amitriptyline (n = 27) or VU992 (n = 66). PSS or DMSO as a vehicle control shown in grey. One Way RM ANOVA, $*P < 0.05$. (c) Confocal images of $Fluo8^{HT}$-stained $mCCD_{cl1}$ cells acquired before and after application of VU992 with the corresponding graph plotting the time course of VU992-induced intracellular calcium transient pooled from ten cells. (d) Summary graph for the peak $Fluo8^{HT}$ fluorescence intensity following application of fluoxetine (n = 40), 3 μM VU992 (n = 40), 30 μM VU992 (n = 95), and amitriptyline (n = 28). PSS or DMSO as a vehicle control shown in grey. One Way ANOVA, Tukey post-hoc test, $*P < 0.05$ compared to vehicle, fluoxetine, and 3 μM VU992. Scale bar is 20 μm.

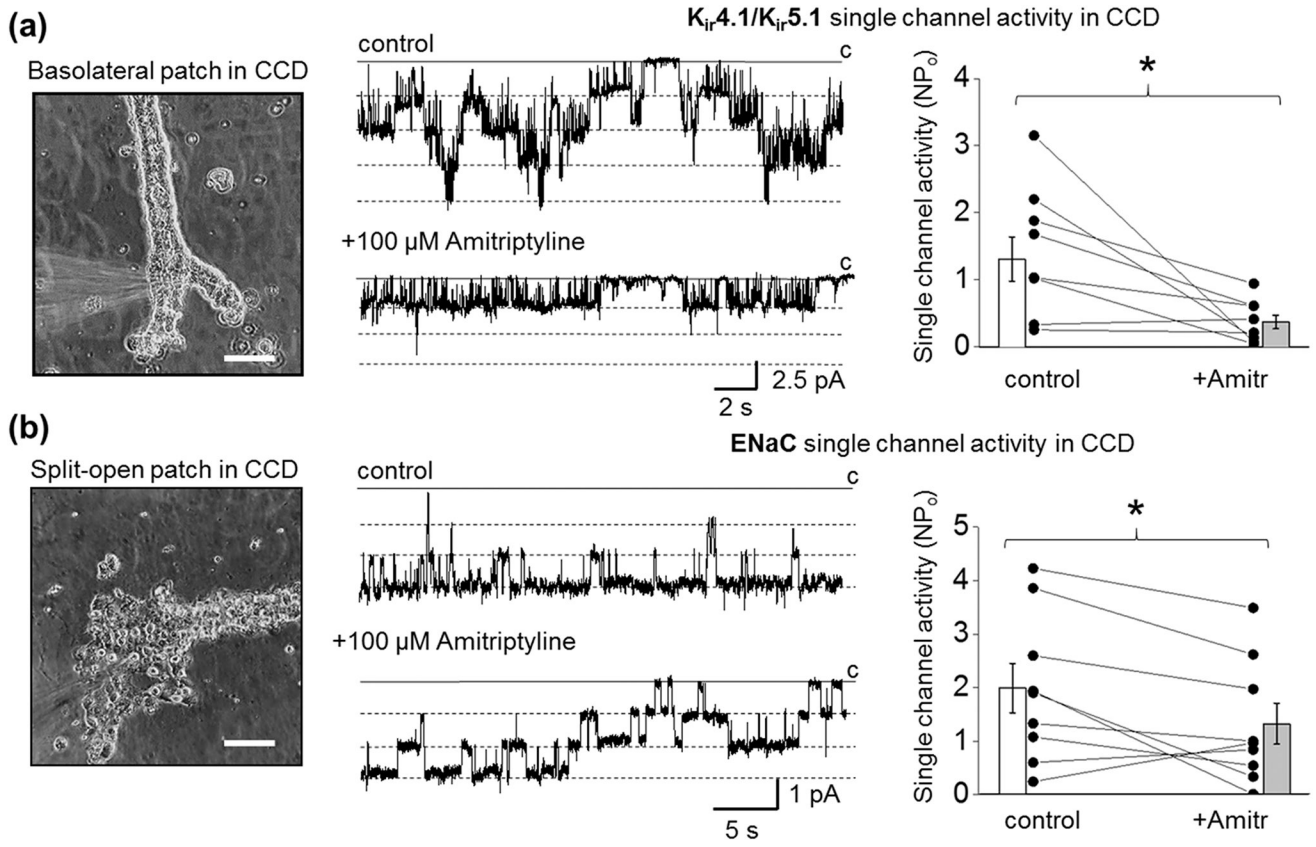

FIGURE 5.

Effect of amitriptyline on $K_{ir}4.1/K_{ir}5.1$ and ENaC single-channel activity in principal cells of freshly isolated rat CCD. Representative patch-clamp configurations (glass pipette forming a giga-seal contact) and corresponding recordings of basolateral $K_{ir}4.1/K_{ir}5.1$ (a) and apical (split-open tubule) ENaC (b) single-channel activity recorded from the CCD principal cells after application of PSS as a vehicle control or application of amitriptyline. Scale bars are 100 μm. Patches were clamped to -Vp = −60 mV. Summary graphs of changes in channel's activity for $K_{ir}4.1/K_{ir}5.1$ (n = 8) and ENaC (n = 9) channels are shown on the right. Paired sample t-test $*P < 0.05$.

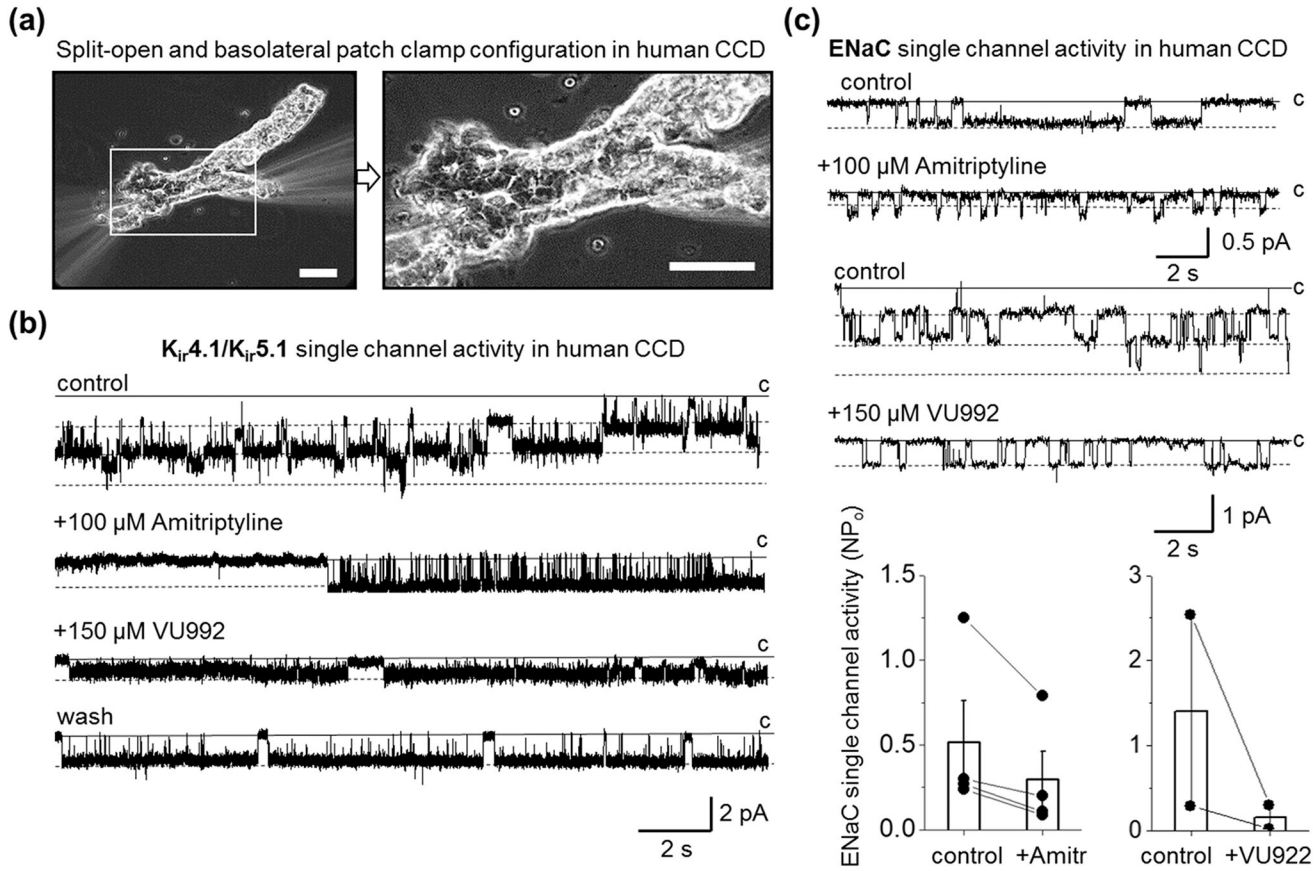

FIGURE 6.

Inhibition of basolateral $K_{ir}4.1/K_{ir}5.1$ channel modulates ENaC activity in human CCD principal cells. (a) Representative image of patch-clamp configuration on apical (split-open) or basolateral parts of freshly isolated human CCD. Scale bars are 40 μm. (b) Representative current traces monitoring basolateral $K_{ir}4.1/K_{ir}5.1$ single-channel activity in cell-attached mode after application of PSS or DMSO as vehicle control or amitriptyline (100 μM) and subsequent addition of VU992 (150 μM). The patch was clamped to -Vp = −60 mV. The single-channel conductance of the recorded channel was 54 pS. Note that the effect of the application of VU992 was reversible (wash). (c) Representative current traces monitoring ENaC single-channel activity after application of PSS or DMSO as a vehicle control or amitriptyline (upper panel; -Vp = −40 mV) or VU992 (bottom; -Vp = −60 mV) applications. A solid line denotes a non-conducting closed state. Dash lines indicate open states. Summary graphs of changes in ENaC activity in response to amitriptyline (n = 4) and VU992 (n = 2) application are also shown.

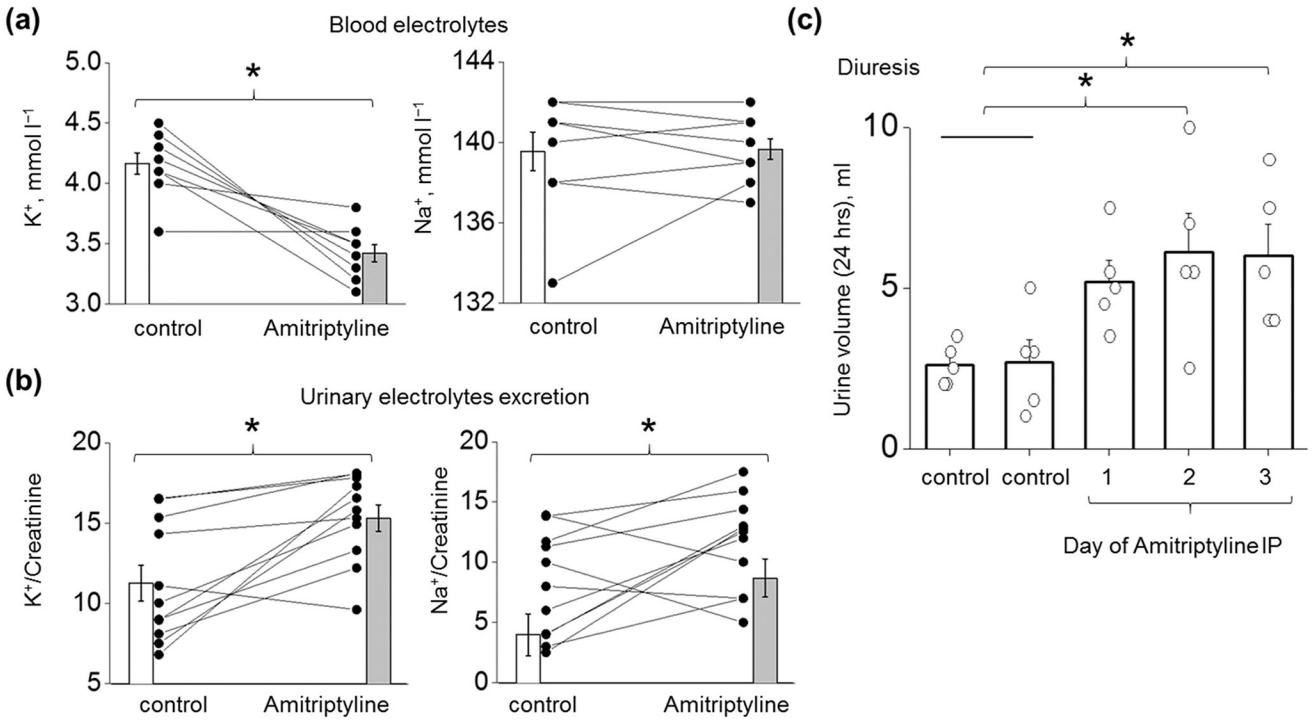

FIGURE 7.

Effect of amitriptyline on sodium/potassium homeostasis in SS rats. (a, b) Biochemical analyses of K^+ and Na^+ in blood (n = 9 for both groups) and urine samples (n = 11 for both groups) collected from SS rat in control (vehicle injection) and after 3 days of consecutive IP injections of amitriptyline (15 mg kg^{-1} day^{-1}). Concentrations of electrolytes in urine were normalized to creatinine (24 hrs collections). Paired sample t-test *$P < 0.05$. (c) Daily urine output in rat injected with vehicle (double control, two or one days before the drug injection) and 15 mg kg^{-1} amitriptyline (n = 5, One Way RM ANOVA with a Greenhouse-Geisser correction ($F(1.56, 6.24) = 5.43$, $P < 0.05$), post hoc test using Dunnett correction *$P < 0.05$ compared to control).

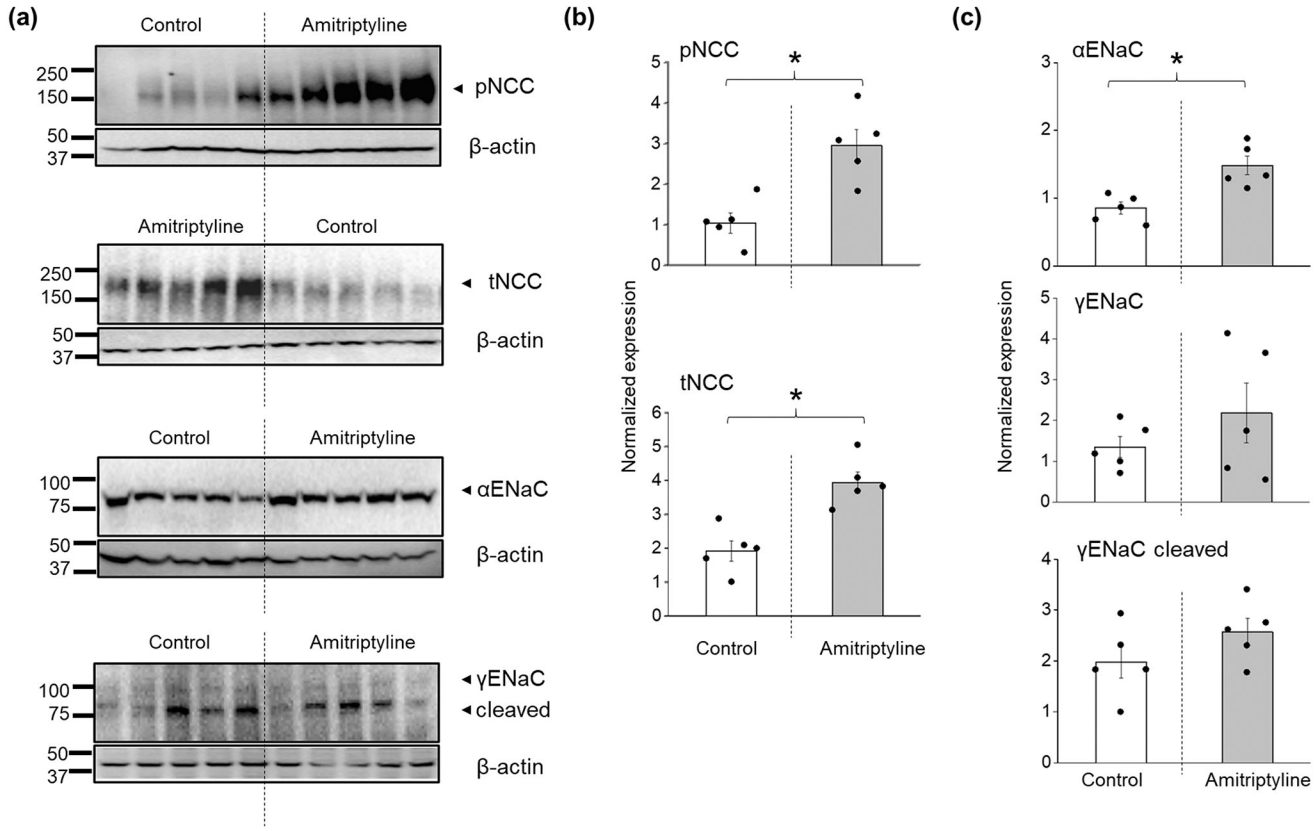

FIGURE 8.

Differences in NCC and ENaC expression in SS rats treated with amitriptyline. (a) Western blotting analysis of tNCC, pNCC, αENaC, cleaved and noncleaved γENaC subunits from the kidney cortex lysates of SS rats under control or after 3 days of i.p. injection with amitriptyline. (b, c) Summary graphs showing the average relative density of the bands (normalized to loading controls) in the studied groups (n = 5 per each group, ANOVA, $*P < 0.05$).